

Solvent coarsening around colloids driven by temperature gradients

Sutapa Roy,^{1,2} S. Dietrich,^{1,2} and Anna Maciolek³

¹*Max-Planck-Institut für Intelligente Systeme,
Heisenbergstr. 3, 70569 Stuttgart, Germany*

²*IV. Institut für Theoretische Physik, Universität Stuttgart,
Pfaffenwaldring 57, 70569 Stuttgart, Germany*

³*Institute of Physical Chemistry, Polish Academy of Sciences,
Kasprzaka 44/52, PL-01-224 Warsaw, Poland*

(Dated: December 22, 2017)

Abstract

Using mesoscopic numerical simulations and analytical theory we investigate the coarsening of the solvent structure around a colloidal particle emerging after a temperature quench of the colloid surface. Qualitative differences in the coarsening mechanisms are found, depending on the composition of the binary liquid mixture forming the solvent and on the adsorption preferences of the colloid. For an adsorptionwise neutral colloid, as function of time the phase being next to its surface alternates. This behavior sets in on the scale of the relaxation time of the solvent and is absent for colloids with strong adsorption preferences. A Janus colloid, with a small temperature difference between its two hemispheres, reveals an asymmetric structure formation and surface enrichment around it, even if the solvent is within its one-phase region and if the temperature of the colloid is above the critical demixing temperature T_c of the solvent. Our phenomenological model turns out to capture recent experimental findings according to which, upon laser illumination of a Janus colloid and due to the ensuing temperature gradient between its two hemispheres, the surrounding binary liquid mixture develops a concentration gradient.

Coarsening is a paradigmatic example for non-equilibrium dynamics of systems approaching a steady state. Typically, this process is induced by a temperature quench of an initially homogeneous two-phase system, such as binary liquid mixture, polymer mixture, into the regime of immiscibility. The dynamics of coarsening, which has been studied intensively for the bulk fluid [1, 2], is changed substantially by the presence of surfaces. In this latter context, a lot of attention has been paid to binary fluids in contact with planar surfaces in semi-infinite or film geometries. Strong efforts have been devoted to phase-separation guided by the surface, which occurs if – as it is generically the case – the surface prefers one species of the binary fluid over the other. Under such conditions, upon a temperature quench of an initially homogeneous system into the miscibility gap, plane composition waves propagate from the surface into the bulk and result in a transient layer structure [3]. There are numerous studies of this, so-called, surface-directed phase-separation process [4, 5]. Most of them assume that after a quench the system – including its boundaries – thermalize instantaneously so that the coarsening proceeds at constant temperature everywhere. Instead of quenching one can apply temperature gradients, e.g., by heating or cooling the boundary of a system. There is much less theoretical work concerning phase separation induced by temperature gradients, inspite of such conditions being created in various experiments and for practical applications, e.g., in polymer systems [6–10]. So far, the focus has been on systems bounded by “planar” and “neutral” surfaces (i.e., with no preference for either component of a two-phase system), supplemented with boundary conditions which maintain a *stationary* linear temperature gradient across a film [9–12]. The effects associated with a temperature quench of a boundary, whereupon the temperature gradient across the system varies in time, has rarely [13, 14] been considered, albeit for a planar geometry. To the best of our knowledge, in this context the effects due to spatio-temporal temperature gradients in fluids bounded by non-neutral surfaces, i.e., in the generic presence of surface fields, have not yet been explored.

Here we consider a spherical colloid suspended in a near-critical binary solvent, kept in its mixed phase above T_c . We study the dynamics of solvent coarsening following a temperature quench of the surface of the suitably coated colloid. Our interest in this problem has been triggered by recent experiments with a partially gold-capped Janus colloid suspended in a mixed phase of water-lutidine mixture below its lower critical point [15, 16] in which, upon laser illumination with sufficient intensity, one observes phase separation of the solvent around the particle. The *early* stage dynamics of this complex process has not yet been investigated. A steady state occurring at *late* times has been considered in the studies of moving Janus colloids for quenches crossing the binodal [17, 18]. In these studies the assumption has been made that the order parameter starts to evolve only after the stationary temperature profile has been reached. Here, we consider the *simultaneous* time evolution of the coupled order parameter and temperature fields. This is expected to have repercussions for the motion of the Janus colloids¹. For homogeneous colloids we observe a surprising pattern evolution, which cannot be captured by the above assumption. For Janus particles we show that, unexpectedly, also temperature quenches, which **do not** cross the binodal, lead to coarsening.

We employ a phenomenological model, which we treat numerically and analytically. Specifically, we use the Cahn-Hilliard-Cook (CHC) type description, based on the Landau-Ginzburg free energy

¹ Allowing for the simultaneous evolution of coupled temperature and OP fields revealed that the body force exerted on a colloid due to the concentration flux is much stronger at the beginning of the coarsening process than in the stationary state. This suggests that the motion of the Janus particle may start before the stationary state is achieved.

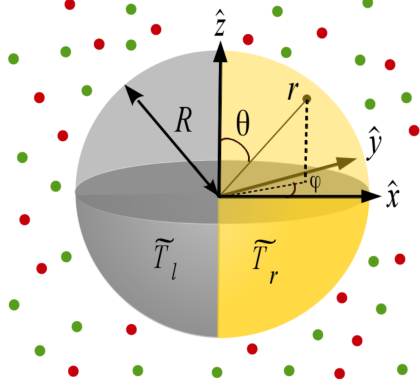


FIG. 1. Spherical Janus colloid of radius R with reduced temperatures \tilde{T}_r and \tilde{T}_l on its right and left hemisphere, respectively. The azimuthal angle φ is measured from the x -axis in the horizontal $\hat{x} \hat{y}$ midplane of the colloid, the polar angle θ is measured from the z axis, and r is the radial distance from the centre. The initial temperature in the whole binary solvent is $\tilde{T}_i = \tilde{T}_r$.

functional conjoined with the heat diffusion equation [1, 13]:

$$\frac{\partial \psi(\mathbf{r}, t)}{\partial t} = \nabla^2 \left(\frac{\tilde{T}(\mathbf{r}, t)}{|\tilde{T}_1|} \psi(\mathbf{r}, t) + \psi^3(\mathbf{r}, t) - \nabla^2 \psi(\mathbf{r}, t) \right) + \eta(\mathbf{r}, t), \quad (1a)$$

$$\frac{\partial \tilde{T}(\mathbf{r}, t)}{\partial t} = \mathcal{D} \nabla^2 \tilde{T}(\mathbf{r}, t). \quad (1b)$$

Here $\psi(\mathbf{r}, t)$ is the local order parameter (OP) and $\tilde{T}(\mathbf{r}, t)$ is proportional to the reduced temperature field $(T(\mathbf{r}, t) - T_c)/T_c$. T_1 is the quench temperature of the colloid surface. The Gaussian random noise obeys the relation $\langle \eta(\mathbf{r}, t) \eta(\mathbf{r}', t') \rangle = -2\nu(\mathbf{r}) \nabla^2 \delta(\mathbf{r} - \mathbf{r}') \delta(t - t')$; $\nu(\mathbf{r})$ is the strength of noise. Equation (1) is valid for phase separation driven by diffusion, with hydrodynamic effects being irrelevant (e.g., for small Péclet numbers or at the early time of coarsening). $\mathcal{D} = D_{th}/(|\tilde{T}_1|D_m)$ involves the ratio of the thermal diffusivity D_{th} of the solvent and the solvent interdiffusion constant D_m . Equation (1) has to be complemented by boundary conditions (b.c.) on the surface \mathcal{S} of the colloid. At a homogeneous surface the temperature field is constant, $\tilde{T}(\mathbf{r})|_{\mathcal{S}} = \tilde{T}_1$, and we assume there is no heat flux through the colloid. The generic preference of the colloid surface for one of the two components of the binary mixture is accounted for by the so-called Robin b.c. $(\hat{n} \cdot \nabla \psi(\mathbf{r}) + \alpha \psi(\mathbf{r}))|_{\mathcal{S}} = h_s$ [19]. Here, α and h_s are the dimensionless surface enhancement parameter and symmetry breaking surface field, respectively. The second necessary b.c. [20] is for no particle flux normal to the surface. Figure 1 explains various notations. The spherical colloid of radius R is placed at the center of a cubic simulation box (SB) with side length L and periodic boundary conditions [21] at the side walls of SB. (For details concerning the model, numerical techniques, and relation to experimentally relevant quantities see SM).

We first study demixing near a homogeneous colloid ($h_s = \text{constant}$ and $\tilde{T}_l = \tilde{T}_r = -1$) quenched from $\tilde{T}_i = 1$ to -1 . Figure 2(a) portrays a typical temperature profile in the midplane at an early time $t = 10$. There is a strong temperature gradient, with $\tilde{T}(\mathbf{r})$ near the side walls of SB being close to the initial value. As demonstrated in Figs. 2 and 3 in SM, this gradient reduces with time until the concentration profile attains a sinusoidal stationary state.

In Fig. 2(b), we show a cross-sectional ($\hat{x} \hat{y}$) view of the evolution patterns at six times. As the solvent cools a layered structure, consisting of concentric circular shells, forms near the colloid. Two neighboring layers contain opposite phases while the phase next to the colloid is $\psi > \psi_0$.

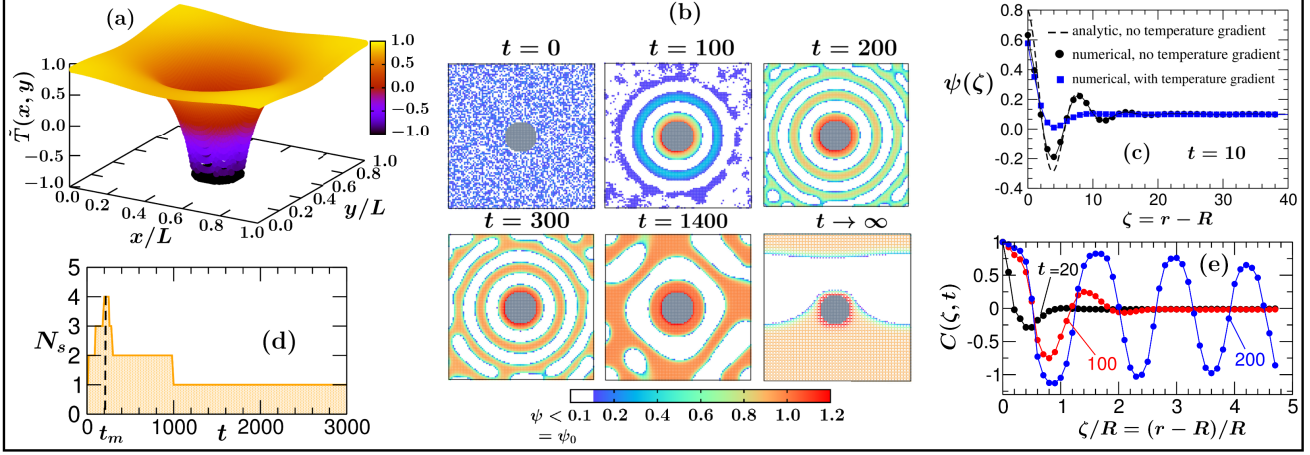


FIG. 2. Temperature-gradient induced demixing around a homogeneous colloid immersed in a binary solvent with off-critical concentration $\psi_0 = 0.1$ and undergoing slow cooling below T_c . The results in (a),(b),(d), and (e) correspond to $L = 100$, $R = 10$, $\alpha = 0.5$, $h_s = 1$, $\mathcal{D} = 50$, and $\nu = 10^{-4}$. (a) Temperature profile in the midplane $z = L/2$ at an early time $t = 10$, exhibiting a strong gradient. Initially, the solvent is hot and the colloid is cold. (b) Coarsening patterns in the midplane of the colloid. Close to the colloid disconnected concentric circular structures form; away from the colloid spinodal-like patterns prevail. As time progresses the shells propagate into bulk via the formation of new layers. As expected, in the long time limit the system forms a planar interface trapping the colloid. (c) Comparison of the approximate analytic prediction of the OP profile without any temperature gradient ((\bullet)) and numerical data (\blacksquare) with a temperature gradient, for $R = 10$, $\tilde{T}_i = 1$, $\alpha = 0.01$, $h_s = 0.1$, and $\nu = 10^{-4}$. (d) Non-monotonic time dependence of the number of concentric shells N_s ; the decrease is much slower than the increase. (e) Radial two-point equal time correlation function $C(\zeta, t)$ vs. reduced distance ζ/R for three values of t . $C(\zeta, t)$ decays spatially fast at early times while with increasing time it develops multiple minima corresponding to concentric shell-like layers around the colloid. Data have been averaged over 10 independent initial configurations.

Away from the colloid spinodal-like patterns prevail (see $t = 100$). Upon increasing time, the shell structure propagates into bulk via formation of new layers and the maximal absolute value of the angularly averaged concentration in each layer increases (see Fig. 2 in SM).

Since a reliable analytic expression for OP in the presence of temperature gradients could not yet be obtained, numerical results are indispensable. In Fig. 2(c), we present numerical results (\blacksquare) for $\psi(r, t)$ after quenching a homogeneous colloid (not the solvent) to below T_c , i.e., with temperature gradient. The dashed line refers to our solution for linearized approximation of Eq. (1) without noise and temperature gradient, with the approximate form (by including h_s in the calculations in [13, 23]): $\psi(\zeta = r - R, t) \approx \psi_0 + (-\alpha\psi_0 + h_s)/(k_f^3 \sqrt{\pi t})(R/(R + \zeta)) \exp(k_f^4 t - \zeta^2/(16k_f^2 t))(A \cos k_f \zeta - (\zeta/(4k_f^3 t)) \sin k_f \zeta)$, where $A = 1 + (5/(8k_f^4 t))(1 - \zeta^2/(8k_f^2 t))$ with $k_f^2 = (1 - 3\psi_0^2)/2$ characterizing the fastest growing mode. Numerical data with temperature gradient (\blacksquare) exhibit smaller peak compared to overall quench. The reason is: in case of a gradient temperature fronts propagate from colloid into bulk slowly and thus coarsening proceeds slowly. Thereby, at $t = 10$, while the OP profile for an overall quench has already developed two prominent minima, for cooling it has acquired only one minimum the absolute value of which is also smaller.

Once the layers spread throughout the system they start to break up (see $t = 1400$ in Fig. 2(b)). The non-monotonic behavior of the number of concentric shells $N_s(t)$ in Fig. 2(d) indicates a novel

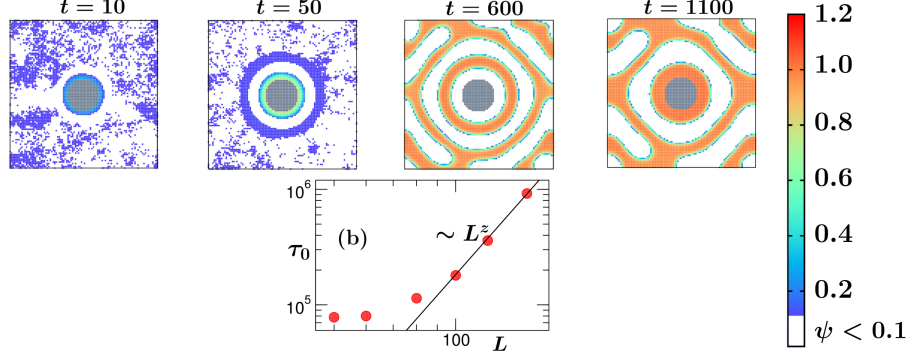


FIG. 3. (a) Snapshots of a cooling binary solvent ($\psi_0 = 0.1$) around an adsorption-neutral, homogeneous colloid. At early times the phase $\psi > \psi_0$ is formed near the colloid surface until at $t \simeq 600$ the phase near the surface is replaced by the one with $\psi < \psi_0$. Results correspond to $L = 100$, $R = 10$, $\tilde{T}_1 = -1 = \tilde{T}_l = \tilde{T}_r$, $\alpha = 0$, $h_s = 0$, and $\nu = 10^{-4}$. (b) Plot of the crossover time τ_0 vs. system size L for $R = 5$. Solid line drawn through the rightmost data points refers to the finite-size critical relaxation time $\propto L^z$; $z = 4$ (see main text).

coarsening mechanism, likely due to an interplay of surface and bulk demixing. The growth and the decay of $N_s(t)$ are not symmetric about the time t_m at which N_s peaks; the break-up is slower.

In order to further investigate the surface patterns around the colloid, we compute the radial two-point equal time correlation function in the midplane defined as $C(\zeta = r - R, t) = \langle \psi(R, t)\psi(R + \zeta, t) \rangle - \langle \psi(R, t) \rangle \langle \psi(R + \zeta, t) \rangle$. The symbol $\langle \cdot \rangle$ denotes the average over initial configurations of the angularly averaged $C(\zeta, t)$. For self-similar domains in bulk, $C(r, t)$ exhibits scaling [22]: $C_{\text{bulk}}(r, t) = \mathcal{C}(r/\ell(t))$, where \mathcal{C} is for bulk and static equilibrium. $\ell(t)$ is mean domain size. In Fig. 2(e), $C(\zeta, t)$ is plotted vs. distance ζ/R , for three t . While at early times $C(\zeta, t)$ decays spatially faster, upon increasing time spatial decay becomes less steep and $C(\zeta, t)$ develops multiple peaks corresponding to various surface layers. However, we could not find any data collapse for $C(r, t)$ onto a function of a single variable. This indicates *non* self-similarity of coarsening patterns due to symmetry-breaking surface fields.

We have explored also the coarsening process around an adsorption-neutral colloid ($\alpha = 0$, $h_s = 0$). For an off-critical solvent, the qualitative feature of the coarsening patterns for a neutral colloid (Fig. 3(a)) is similar to that with surface adsorption preferences (Fig. 2(b)). However, there is a difference concerning the phase formed at the colloid surface. While for $h_s > 0$ the phase with $\psi > \psi_0$ remains at the surface at all times, for the neutral colloid a crossover occurs: at very early times the phase $\psi > \psi_0$ is dominant near the surface until the layered structures have spread throughout the system and beyond a crossover time τ_0 ($t = 600$ in Fig. 3(a)) the phase $\psi < \psi_0 = 0.1$ is formed near the surface. We anticipate this first crossover time τ_0 to be proportional to the OP relaxation time τ [24] of the solvent. For a near-critical system $\tau \propto \xi^z$; ξ being the equilibrium bulk correlation length. Thus for a finite system at $T_{c,\text{bulk}}$ it scales as $\tau \propto L^z$ [25]; $z \simeq 4$ is the dynamic critical exponent for model B [25] with diffusive dynamics for conserved order parameter (Eq. (1a)). In Fig. 3(b) data for τ_0 are plotted for various system sizes. Agreement with the aforementioned power-law behavior (solid line) on a double-logarithmic scale supports the expectation $\tau_0 \sim \tau$. Such a crossover is observed only for neutral colloids, for off-critical concentrations, and for simultaneous time evolution of coupled OP and temperature fields. For the time evolution of the OP with stationary temperature profiles or for critical concentration, always both phases form near the surface and the OP morphology is not shell-like.

Next, we turn to coarsening of solvent around a *Janus* colloid with two hemispheres at different

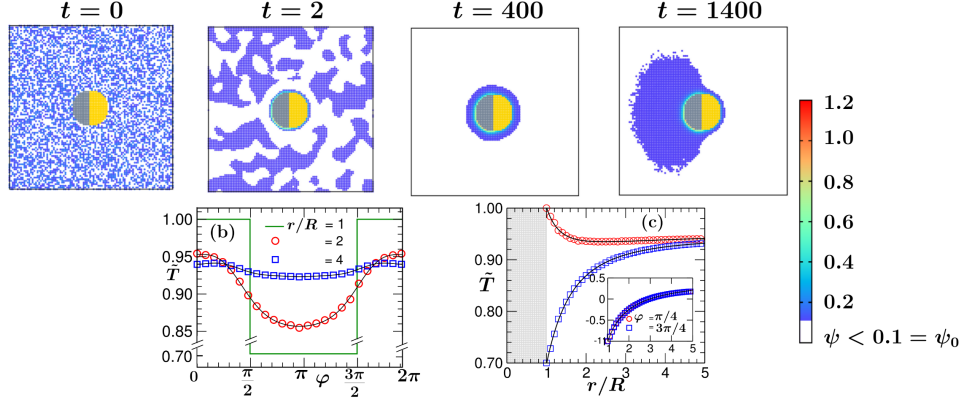


FIG. 4. Coarsening of a binary solvent with $\psi_0 = 0.1$ around a Janus colloid. Results correspond to $L = 100$, $R = 10$, $\alpha = 0.5$, $h_{s,l} = 1$, $h_{s,r} = 0.5$, and $\nu = 10^{-5}$. (a) Evolution patterns in its midplane ($\theta = \pi/2$). The left and right hemispheres are grey and yellow, respectively. Initially, both the solvent and colloid are at $\tilde{T} = 1$. From $t = 1$ to 400 the system evolves at constant temperature everywhere. At $t = 401$ the temperature of the left hemisphere is quenched to $\tilde{T}_l = 0.7$. The corresponding stationary configuration is shown at $t = 1400$. Although both hemispheres are maintained above T_c , structure formation is observed. (b) Temperature distribution $\tilde{T}(r, \varphi) > 0$ of the solvent in the midplane around a Janus colloid. Dependence (b) on the azimuthal angle φ for two radial distances r from the colloid centre and (c) on r for two opposite angles φ corresponding to the right and to the left hemisphere, respectively. The shaded region in (c) corresponds to the space occupied by the colloid. Inset of (c): as in main frame, but for the homogeneous colloid discussed in Fig. 2 for which there is no dependence on φ .

temperatures; both hemispheres prefer the same component of the solvent but with different strengths. Figure 4(a) shows OP distributions. We start with a homogeneous configuration of the binary solvent at $\tilde{T} = 1$ and keep both hemispheres of the Janus colloid at $\tilde{T} = 1$ (above T_c) at $t = 0$. Subsequently, we let the system evolve ($t = 1$ to 400) such that there is no temperature gradient. Accordingly, the surface enrichment phenomenon is the only mechanism for structure formation. The snapshot at $t = 400$ corresponds to the equilibrium surface adsorption OP profile. The Janus character of the colloid causes only weak deviations from a spherically symmetric adsorption profile. Next, at $t = 401$ we quench the left hemisphere of the Janus colloid to $\tilde{T} = 0.7$ such that the subsequent evolution will occur in the presence of a temperature gradient. The corresponding stationary configuration is shown at $t = 1400$. The comparison of the snapshots at $t = 400$ and $t = 1400$ clearly demonstrates the difference between the equilibrium surface pattern formed due to surface enrichment only and the steady state pattern emerging in the presence of a temperature gradient. Clearly, a temperature gradient leads to a more pronounced bubble formation on the cold side of the Janus colloid. Coarsening in fluid regions with $T > T_c$ was observed experimentally [6] in polymer solutions due to the Soret effect and numerically [14] in fluid mixtures due to convective flows. Here, for *purely diffusive* dynamics, i.e., without involving any hydrodynamic flow, we observe the condensation of a droplet around the colloid above T_c , which is a novel phenomenon due to the combination of Soret and surface effects. To relate the anisotropy of surface patterns with temperature gradients, within the midplane we have computed the radial and angular dependence of \tilde{T} on r and φ , respectively. Figure 4(b) depicts the dependence of \tilde{T} on φ for two fixed values of r with temperature in stationary state. The symbols correspond to our numerical data; the solid lines refer to analytical predictions [26]: $\tilde{T}(r, \varphi) = A_0 + \sum_{n=0}^{\infty} B_n P_n(\cos \varphi) (R/r)^{n+1}$, where B_n are

constants and $\{P_n\}$ Legendre polynomials. In Fig. 4(c) we plot the radial dependence of \tilde{T} for two opposite angles. Our numerical results agree with the theoretical predictions. The very slow (algebraic) decay of stationary temperature profile facilitates coarsening in extended regions of the system; in our simulation box it takes place everywhere. Due to finite size, away from the colloid \tilde{T} is lower than its initial value. Note that $\tilde{T}(r, \varphi)$ is anisotropic, i.e., different for the two angles considered. This should be compared with the homogeneous colloid for which $\tilde{T}(r)$ is radially symmetric (see inset of Fig. 4(c)) and coarsening patterns are also symmetric (Fig. 2(b)). This confirms anisotropy of the temperature distribution to be the dominant source of the anisotropy in OP distribution around a Janus colloid. Upon increasing radius of the colloid, the radial extent of a stationary bubble of the phase preferred by the colloid and the amplitude of the OP profile increase moderately. The value of the OP at the left hemisphere surface is slightly larger than at a planar wall ($R \rightarrow \infty$). At the right hemisphere it is reduced to about half the value for planar wall. Interestingly, we find that the OP autocorrelation functions with time-dependent temperature gradients decay slower than in the case of the stationary temperature profiles.

In summary, the simultaneous time evolution of the coupled order parameter and temperature fields leads to new transient patterns. For deep quenches (corresponding to $\mathcal{D} \approx 100$), the time scale of patterns for a molecular solvent varies between 10^{-1} s and 10^{-2} s, depending on the size of the colloid and simulation box (see SM). There is anisotropic structure formation around a Janus colloid even if the colloid and the solvent are at temperatures corresponding to its one-phase region, which is different from *surface enrichment* [4, 27, 28]. The former situation might have occurred in experiments in Ref. [15, 16] for low intensity illuminations. Even if $\tilde{T}(\mathbf{r}, t)$ exhibits a fast dynamics, the results of our study are relevant for controlling pattern formation, e.g., in polymers, using hot homogenous or Janus particles [29]. It is expected that the transient dynamics crucially influences the final patterns; these patterns should definitely be different from those seen for spatially homogeneous quenches. Our study contributes to the understanding of the propulsion mechanism via diffusive dynamics for one of the commonly used representatives of synthetic active matter [15, 16] (see (1)). The other presently available theoretical approaches [17, 18] are based instead on hydrodynamics and are complementary to our study. Generally, dipping a particle into its binary solvent causes transportation of the preferred phase towards its surface. From our study we conclude that this transport is strongly enhanced if supported by a time-dependent temperature gradient.

Acknowledgments: The work by AM has been supported by the Polish National Science Center (Harmonia Grant No. 2015/18/M/ST3/00403).

-
- [1] A.J. Bray, *Adv. Phys.* **43**, 357 (1994).
 - [2] K. Binder, in *Kinetics of Phase Transitions*, edited by S. Puri and V. Wadhawan (CRC, Boca Raton, 2009), p. 62.
 - [3] S. K. Das, S. Puri, J. Horbach, and K. Binder, *Phys. Rev. Lett.* **96**, 16107 (2006).
 - [4] S. Puri, *J. Phys.: Condens. Matter* **17**, R1 (2005).
 - [5] H. Tanaka, *J. Phys.: Condens. Matter* **13**, 4637 (2001).
 - [6] J. Kumaki, T. Hashimoto, and S. Granick, *Phys. Rev. Lett.* **77**, 10 (1996).
 - [7] J. K. Platten and G. Chavepeyer, *Physica A* **231**, 110 (1995).
 - [8] Q. Tran-Cong and J. Okinaka, *Polym. Eng. Sci.* **39**, 365 (1999).
 - [9] P. K. Jaiswal, S. Puri, and K. Binder, *EPL* **103**, 66003 (2013).

- [10] H. Jiang, N. Dou, G. Fan, Z. Yang, and X. Zhang, *J. Chem. Phys.* **139**, 124903 (2013).
- [11] G. Gonella, A. Lamura, and A. Piscitelli, *J. Phys. A* **41**, 105001 (2008).
- [12] S. Hong and P. K. Chan, *Model. Simul. Mater. Sci. Eng.* **18**, 025013 (2010).
- [13] R.C. Ball and R.L.H. Essery, *J. Phys.: Condens. Matter* **2**, 10303 (1990).
- [14] T. Araki and H. Tanaka, *EPL* **65**, 214 (2004).
- [15] G. Volpe, I. Buttinoni, D. Vogt, H.J. Kammerer, and C. Bechinger, *Soft Matter* **7**, 8810 (2011).
- [16] J.R. Gomez-Solano, A. Blokhuis, and C. Bechinger, *Phys. Rev. Lett.* **116**, 138301 (2016).
- [17] A. Würger, *Phys. Rev. Lett.* **115**, 188304 (2015).
- [18] S. Samin and R. van Roij, *Phys. Rev. Lett.* **115**, 188305 (2015).
- [19] H. W. Diehl, *Int. J. Mod. Phys. B* **11**, 3503 (1997).
- [20] H. W. Diehl and H. K. Janssen, *Phys. Rev. A* **45**, 7145 (1992).
- [21] M.P. Allen and D.J. Tildesley, *Computer Simulations of Liquids* (Clarendon, Oxford, 1987).
- [22] S. Roy and S.K. Das, *Soft Matter* **9**, 4178 (2013); *J. Chem. Phys.* **139**, 044911 (2013).
- [23] B. P. Lee, J. F. Douglas, and S. C. Glotzer, *Phys. Rev. E* **60**, 5812 (1999).
- [24] J.-P. Hansen and I. R. McDonald, *Theory of Simple Liquids* (Academic, London, 2008).
- [25] R. Folk, and G. Moser, *J. Phys. A: Math. Gen.* **39**, R207 (2006).
- [26] T. Bickel, A. Majee, and A. Würger, *Phys. Rev. E* **88**, 012301 (2013).
- [27] R. A. L. Jones, E. J. Kramer, M. H. Rafailovich, J. Sokolov, and S. A. Schwarz, *Phys. Rev. Lett.* **62**, 280 (1989).
- [28] S. Puri and H. L. Frisch, *J. Chem. Phys.* **79**, 5560 (1993).
- [29] R. Kurita, *Scien. Rep.* **7**, 6912 (2017).